

# Model for a Thulium-Doped Silica Fiber Amplifier Pumped at 1558 nm and 793 nm

M A Khamis, K Ennsner

**Abstract**—This paper investigates the static behavior of Thulium-doped fiber amplifier (TDFA) operating around 2 μm at two different pump wavelengths. The developed model provides the influences of the amplified spontaneous emission (ASE) noise, the wavelength and the power of the seed, the thulium-doped fiber length and the pumping power into the TDFA. Simulation results show that the amplifier with pump at 1558 nm is more efficient than one with pump at 793 nm with core pumped low concentration thulium-doped silica fiber. Our findings reveal that a larger amplified signal can be achieved by increasing the pump power and the thulium-doped fiber length. In case of in-band pumping, the maximum gain reaches up to 34.4 dB with a 2 W pump power when a -10 dBm seed wavelength at 1900 nm is used. In contrast to indirect pumping, only 30 dB maximum gain is achieved under the same conditions. Also, it is important to take into account the selection of the seed wavelength in the TDFA design because high amplification can be produced when the selection seed wavelength is near the center of the emission cross-section curve

**Index Terms**— Amplified spontaneous emission, cross-relaxation process, silica glass material, Thulium-doped fiber amplifier.

## I. INTRODUCTION

Throughout the past few years, eye-safe fiber laser sources around 2 μm have become an attractive technology for a large number of potential applications; for example: atmospheric measurements, laser radar, longer-wavelength laser pumping, laser plastics material processing, free-space optical communication, gas detection, biomedical and medical applications such as laser angioplasty, ophthalmic procedures, laser lithotripsy, and laser surgeries [1-5]. Very recently the wavelengths around 2 μm have been proposed as a potential new window of data transmission for several reasons. Firstly, the hollow-core photonic band gap offers an ultra-low loss window at 2 μm [6,7]. Secondly, thulium-doped fiber amplifiers (TDFAs) have recently been developed and characterized for optical communications, indicating low noise amplification and high gain in the spectral region [8]. Finally, the emission spectrum of the  $^3F_4 - ^3H_6$  transition in TDFA covers about 30 THz (1700-2100 nm) of amplification bandwidth in a single device (more than two times that of the erbium-doped fiber amplifier (EDFA) with the same configuration and complexity) [9].

To optimize the parameters of practical systems, it is necessary to investigate the characteristics of lasers and amplifiers by using theoretical modeling and simulation. There are a lot of theoretical modeling results published for erbium and ytterbium-doped fiber lasers and amplifiers [10-11]. However, there are only a few papers on the

theoretical modeling and simulation of thulium-doped fiber lasers and amplifiers at 2 μm [12-14]. In addition these models do not consider the effect of the amplified spontaneous emission noise on the performance of the lasers or amplifiers. Moreover there is no fair comparison of the TDFA performance for the different thulium pump schemes at  $^3F_4 - ^3H_6$  transition. Only Jackson [12] has demonstrated that an in-band laser is the best option but determines this without ASE noise effect and not for optical amplifier.

This paper presents a theoretical model of TDFA operating at 2 μm by solving a set of rate and propagation equations for in-band and indirect pumping. The model takes into account the ASE noise, the wavelength and the power of the seed, the thulium-doped fiber length and the pumping power. A MATLAB program is developed to investigate the TDFA performance when the thulium-doped silica fiber is pumped into the  $^3F_4$  (in-band pumping) and into the  $^3H_4$  (indirect pumping) absorption bands.

## II. NUMERICAL MODEL OF TDFA

The amplifier model is based on the rate equation of the electronic excitation in the thulium ions. The atomic rate equations describe the interaction between the pump, the signal and the ASE light in the TDFA. The populations in the energy levels can be estimated from the rate equations under any pump and signal power conditions. According to the chosen pumping scheme, a separate numerical model is constructed based on [12]. The model assumes that only the core of the fiber is pumped.

### A. Modeling for in-band Pumping

The rate equations of the thulium-doped fiber amplifier at any point along the fiber length when the  $^3F_4$  energy level is directly excited are as follows [12,15]:

$$\frac{dN_2(z,t)}{dt} = w_{p12}N_1(z,t) - w_{p21}N_2(z,t) - \frac{N_2(z,t)}{\tau_2} \quad (1)$$

$$- w_{s21}N_2(z,t) + w_{s12}N_1(z,t)$$

$$N_1(z,t) = N_T - N_2(z,t) \quad (2)$$

Where  $\tau_2$  is the spontaneous lifetime of  $^3F_4$  level,  $N_1$  and  $N_2$  are the population densities of the active Thulium ions for  $^3H_6$  and  $^3F_4$  levels respectively,  $N_T$  is the  $Tm^{3+}$  concentration and set to be a constant. And when  $w_{p12}$  is the pumping rate from  $^3H_6$  to  $^3F_4$  and  $w_{p21}$  represents the de-excitation rate of the  $^3F_4$  level,  $w_{s21}$  is the stimulated emission rate from  $^3F_4$  to  $^3H_6$ , and  $w_{s12}$  is the stimulated absorption rate from  $^3H_6$  to  $^3F_4$ . The expressions of  $w_{p12}$ ,  $w_{p21}$ ,  $w_{s21}$  and  $w_{s12}$  are given as follows:

$$w_{p12} = \frac{\lambda_p \Gamma_p}{hcA_{core}} \sigma_a(\lambda_p) [p_p^+(z) + p_p^-(z)] \quad (3)$$

Revised Version Manuscript Received on April 24, 2016.

M A Khamis, Department of Electronic and Electrical, College of Engineering, Swansea University, Swansea, UK.

K Ennsner, Department of Electronic and Electrical, College of Engineering, Swansea University, Swansea, UK.

## Model for a Thulium-Doped Silica Fiber Amplifier Pumped at 1558 nm and 793 nm

$$w_{p21} = \frac{\lambda_p \Gamma_p}{hcA_{core}} \sigma_e(\lambda_p) [p_p^+(z) + p_p^-(z)] \quad (4)$$

$$w_{s12} = \frac{\lambda_s \Gamma_s}{hcA_{core}} \sigma_a(\lambda_s) [p_s(z) + ASE_f(z) + ASE_b(z)] \quad (5)$$

$$w_{s21} = \frac{\lambda_s \Gamma_s}{hcA_{core}} \sigma_e(\lambda_s) [p_s(z) + ASE_f(z) + ASE_b(z)] \quad (6)$$

Where  $h$  is the Planck constant;  $c$  is the light speed in vacuum;  $\lambda_p$  and  $\lambda_s$  are the wavelengths of the pump and the signal in vacuum, respectively;  $\Gamma_p$  and  $\Gamma_s$  are the overlapping vector for the pump and the signal, respectively;  $A_{core}$  is the cross-section area of the fiber core;  $\sigma_a(\lambda_p)$  and  $\sigma_a(\lambda_s)$  are the absorption cross-sections of the pump light and the signal light, respectively;  $\sigma_e(\lambda_p)$  and  $\sigma_e(\lambda_s)$  are the emission cross-sections of the pump light and the signal light, respectively;  $P_p^+(z)$  and  $P_s(z)$  are the pump (corresponding to forward and backward) and the signal power at position  $z$ ;  $ASE_f(z)$  and  $ASE_b(z)$  are the forward and backward amplified spontaneous emission power at position  $z$ . The power distributions of the pump and signal wavelength along the fiber length can be expressed by the following propagation equation:

$$\frac{dp_p^\pm}{dz} = \pm p_p^\pm(z) [\Gamma_p (\sigma_e(\lambda_p) N_2(z) - \sigma_a(\lambda_p) N_1(z)) - \alpha_{p1}] \quad (7)$$

$$\frac{dp_s}{dz} = p_s(z) [\Gamma_s (\sigma_e(\lambda_s) N_2(z) - \sigma_a(\lambda_s) N_1(z)) - \alpha_s] \quad (8)$$

The distribution of the ASE power along the fiber length can be established as follows [16,17]:

$$\frac{dASE_f}{dz} = ASE_f(z) [\Gamma_s (\sigma_e(\lambda_s) N_2(z) - \sigma_a(\lambda_s) N_1(z)) - \alpha_s] + 2\sigma_e(\lambda_s) N_2(z) \frac{hc^2}{\lambda_s^3} \Delta\lambda \quad (9)$$

$$\frac{dASE_b}{dz} = -ASE_b(z) [\Gamma_s (\sigma_e(\lambda_s) N_2(z) - \sigma_a(\lambda_s) N_1(z)) - \alpha_s] - 2\sigma_e(\lambda_s) N_2(z) \frac{hc^2}{\lambda_s^3} \Delta\lambda \quad (10)$$

Where  $\alpha_{p1}$  and  $\alpha_s$  are the intrinsic absorption at the 1558 nm pump and signal wavelength for the Thulium-doped fiber, respectively,  $\Delta\lambda$  is the bandwidth of the amplified spontaneous emission (ASE) at around 2  $\mu\text{m}$ .

### B. Modeling for in direct pumping scheme

When the  $^3\text{H}_4$  thulium energy level is pumped directly, the system of rate equations includes the cross-relaxation mechanism. The general rate equations for the thulium energy levels at any point along the length of the fiber when pumped at 793 nm are given by eq. (11-13) based on Jackson model [12] and under different approximation conditions [18,19]. Our model neglects the influences of the power up conversion process and ignored the energy level  $N_3$  because it is sufficiently small compared to the other levels.

$$\frac{dN_4}{dt} = w_{p14} N_1(z, t) - \frac{N_4(z, t)}{\tau_4} - k_{4212} N_1(z, t) N_4(z, t) + k_{2124} N_2^2 \quad (11)$$

$$\frac{dN_2}{dt} = 2k_{4212} N_1(z, t) N_4(z, t) - 2k_{2124} N_2^2 - w_{s21} N_2(z, t) + w_{s12} N_1(z, t) - \frac{N_2(z, t)}{\tau_2} + \frac{\beta_{42} N_4(z, t)}{\tau_4} \quad (12)$$

$$N_1(z, t) = N_T - N_2(z, t) - N_4(z, t) \quad (13)$$

Where  $k_{1242}$  and  $k_{2124}$  are the cross relaxation constant.  $N_1$ ,  $N_2$  and  $N_4$  are the population densities of the active Thulium ions for  $^3\text{H}_6$ ,  $^3\text{F}_4$  and  $^3\text{F}_6$  levels;  $B_{42}$  is the branching ratio of the spontaneous transition from level 4 to 2. The expressions of  $w_{p12}$ ,  $w_{p21}$ ,  $w_{s21}$ ,  $w_{s12}$  and the power distributions of  $w_{s12}$ ,  $w_{s21}$ ,  $ASE_f$  and  $ASE_b$  can be taken from an in-band pump model. Only the pump power distribution along the fiber length is different because the de-excitation of the  $^3\text{H}_4$  energy level is omitted and can be established as follows [12]:

$$\frac{dp_p^\pm}{dz} = \mp p_p^\pm(z) [\Gamma_p (\sigma_a(\lambda_p) N_1(z)) + \alpha_{p2}] \quad (14)$$

## III. RESULTS AND DISCUSSION

To solve the thulium rate equations for the two models in steady state condition, the time derivatives of eqs. (1) to (2) for in-band pumping and (11) to (13) for in-direct pumping are set to zero. The fourth-order Runge-Kutta method is applied to solve the differential equations of the pump, the signal, and the amplified spontaneous emission ASE signals. Table 1 summarizes all parameters of the SM-TSF-9/125 fiber used in the numerical simulations. Notes that these values are provided from the Nufern fiber supplier. Initially, the entire population is assumed to be at the ground level  $^3\text{H}_6$  in the numerical calculations.

Table 1 Thulium fiber parameters

Symbol	Quantity	Value
$N_T$	Thulium concentration	$1.37 \times 10^{25} \text{ m}^{-3}$
$\tau_2$	Lifetime of level $^3\text{F}_4$	250 $\mu\text{s}$
$\tau_4$	Lifetime of level $^3\text{H}_4$	25 $\mu\text{s}$
$\lambda_{p1}$	In-band pump wavelength	1558 nm
$\lambda_{p2}$	In-direct pump wavelength	793 nm
$\sigma_a(\lambda_{p1})$	Laser absorption cross section at $\lambda_{p1}$	$2.5 \times 10^{-25} \text{ m}^2$ [20]
$\sigma_a(\lambda_{p2})$	Laser absorption cross section at $\lambda_{p2}$	$8.4 \times 10^{-25} \text{ m}^2$ [20]
$\sigma_e(\lambda_{p1})$	Laser emission cross section at $\lambda_{p1}$	$0.2 \times 10^{-25} \text{ m}^2$ [20]
$\sigma_a(\lambda_s)$	Laser absorption cross section at signal wavelength	See Ref [20]
$\sigma_e(\lambda_s)$	Laser emission cross section at signal wavelength	See Ref [20]
$A$	Area cross section of the core	$6.36 \times 10^{-11} \text{ m}^2$
$\Gamma_p$	Pump confinement factor	0.7
$\Gamma_s$	Signal confinement factor	0.7
$\alpha_{p1}$	Intrinsic absorption at the 1558 nm pump wavelength.	$2.5 \times 10^{-2} \text{ m}^{-1}$
$\alpha_{p2}$	Intrinsic absorption at the 793 nm pump wavelength.	$1.99 \times 10^{-3} \text{ m}^{-1}$
$\alpha_s$	Intrinsic absorption at the signal wavelength	$3.9 \times 10^{-2} \text{ m}^{-1}$

Table 2 explains the initial conditions for the pump power, the signal power and the ASE spectrum in forward and backward directions [21]. The thulium-doped fiber with length L is divided into L segments along the z-direction. The solution is applied for the pump, the signal and the ASE power propagating in the first segment (segment 0) by using the above initial conditions. For the following segments (segment 1 to L-1), the power for the pump, the signal and the ASE at one end of a segment is applied as the input for the next segment. Relaxation method is used to solve the differential equations of the pump, the signal and the ASE powers [21]. Using the data of Table 1 and the values of the emission and the absorption cross-section spectra according to [20], we solve numerically the rate equations of the two pump models.

Table 2 Initial conditions for the numerical simulations

Initial condition	Explanation
$P_p^+(z=0)$ = Forward launched pump power	initial condition for 1558 nm and 793 nm pumps at $z=0$ .
$P_p^-(z=L)$ = Backward launched pump power	initial condition for 1558 nm and 793 nm pumps at $z=L$ .
$P_s(z=0)$ = seed power	initial condition for seed power at $z=0$ .
$ASE_f(z=0)=0$	initial condition for forward amplified spontaneous emission at $z=0$ .
$ASE_b(z=L)=0$	initial condition for backward amplified spontaneous emission at $z=L$ .

**A. Optimization of the Fiber Length**

A MATLAB program is developed to evaluate the optimum thulium-doped fiber length for each of the two pumping schemes. Note that only the forward launched pump will be discussed in these simulations. Figure 1 and 2 illustrate the theoretical prediction of the output power and the residual pump power along a 1558 nm and 793 nm core pumped 0.2wt. % thulium-doped silicate fiber amplifier, respectively. The 9 μm diameter fiber core is seeded by a -10 dBm input signal at 1900 nm and launched pump power of 30 dBm. As shown in Fig. 1, the amplifier produces 0.33 W at its optimum length of 4 m when pumped at 1558 nm. Figure 2 indicates that at the same seed and pump power, the indirect pumped amplifier needs 3 m fiber length to produce a maximum signal power of 0.1 W. The in-band pumped amplifier needs a longer length of thulium-doped fiber because the absorption cross-section at pump wavelength of 1558 nm is lower than at 973 nm. As a result, the gain and the amplified spontaneous emission power are high when the pump wavelength is 1558 nm in comparison with the indirect pump case as illustrated in Figs. 3 and 4.

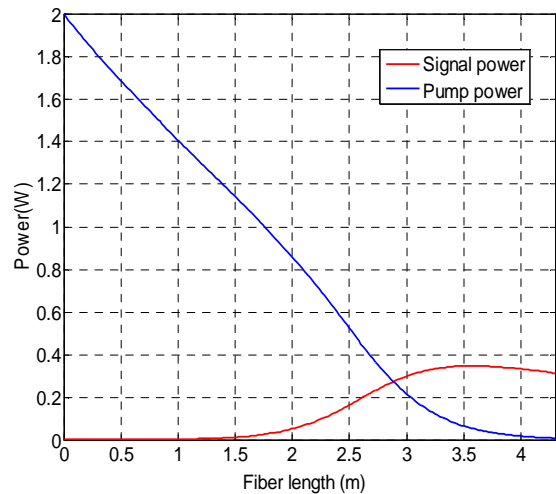


Fig. 1. Output signal at 1900 nm and pump power dependence on fiber length at the launched pump wavelength of 1558 nm

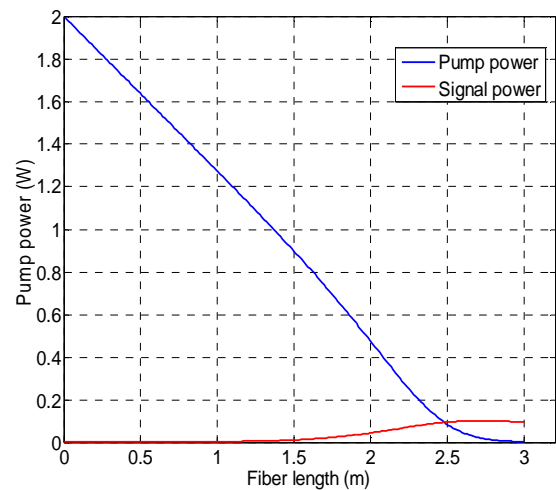


Fig. 2. Output signal at 1900 nm and pump power dependence on fiber length at the launched pump wavelength of 793 nm.

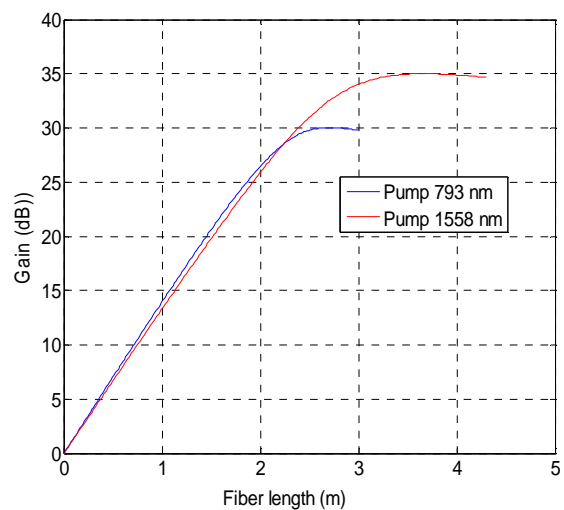


Fig. 3. Signal gain at 1900 nm along the thulium fiber length for the launched pump wavelengths of 1558 nm and 793nm.

# Model for a Thulium-Doped Silica Fiber Amplifier Pumped at 1558 nm and 793 nm

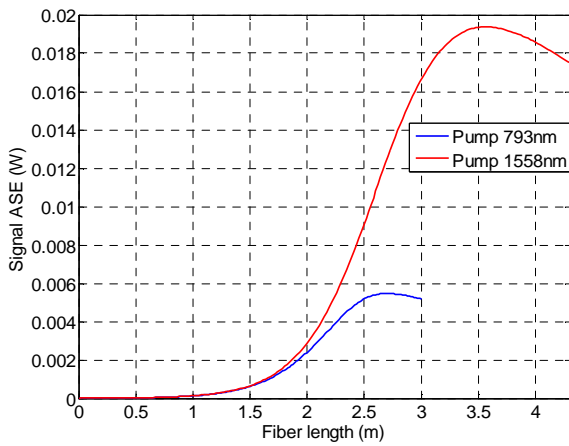


Fig. 4. ASE signal at 1900 nm dependence on fiber length at 1558 nm and 793 nm launched pump wavelengths.

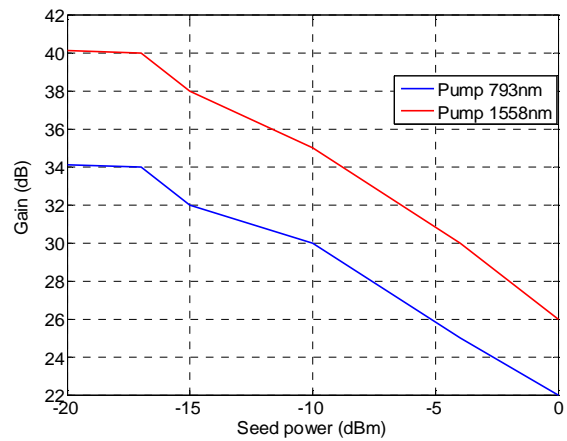


Fig. 6. Signal gain at 1900 nm versus different input signal levels for the launched pump wavelengths of 1558 nm and 793 nm.

## B. The Impact of Pump Power in the Amplifier

The pump powers has a significant influence on the amplifier performance. Figure 5 gives the output gain versus the pump power at two launched pump wavelengths when the seed wavelength is fixed at 1900 nm, the seed power is -10 dBm, and the fiber length is 4.3 m for the pump wavelength at 1558 nm and 3 m for the pump wavelength at 793 nm. It can be seen from the figure that the gain increases almost linearly with the pump power up to 2 W. Notes that after 2 W pump power, the amplifier gain grows slower. Therefore this value of pump power is used as optimized value in our simulations.

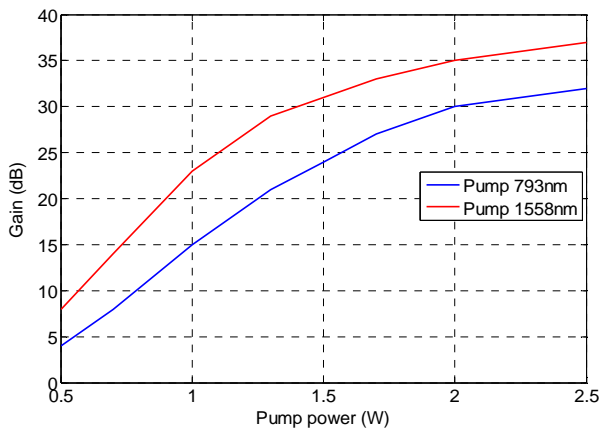


Fig. 5. Signal gain at 1900 nm versus different pump levels for the launched pump wavelengths of 1558 nm and 793 nm.

## C. The Impact of Seed Power in the Amplifier

The performance of the TDFA is also directly affected by the seed power. Figure 6 explains the performance of a gain amplifier with respect to the variation in seed power at 1900 nm and with the fixed launched power at 2 W under different pump power wavelengths. It is clearly apparent that the amplifier reaches saturation after -14 dBm at both pump wavelengths 1558 nm and 793 nm. Thus, the optimized seed power should be selected equal or more than the saturated value in the design of TDFA.

## D. The Impact of Pump Power in the Amplifier

Another important factor that contributes to the TDFA performance is the seed wavelength over the amplification bandwidth. Figure 7 shows the amplifier gain over the seed wavelengths for the two launched pump wavelengths above. Note that the pump and seed power for both cases of pump wavelengths are fixed at 2W and 0.1 mW, respectively. The amplifier gain reaches up to 34.4 dB at 1850 nm when the pump wavelength is 1558 nm. The full width at half-maximum (FWHM) of the gain is 215 nm between 1770 nm to 1985 nm. For the indirect pumping scheme, the maximum gain signal is only 30 dB at 1850 nm and the bandwidth at FWHM is circa 180 nm between 1770 to 1950 nm. The reason for the amplifier gain variation over the seed wavelength is mainly because the emission cross-section reduces rapidly out of these ranges. Figure 8 depicts the noise figure over the seed wavelengths for both pump wavelengths. For values below 1800nm the noise figure for the pump wavelength at 1558 nm is clearly higher than the indirect pumping scheme. Above 1800 nm the noise figure is around 6.3 dB for both pumping schemes.

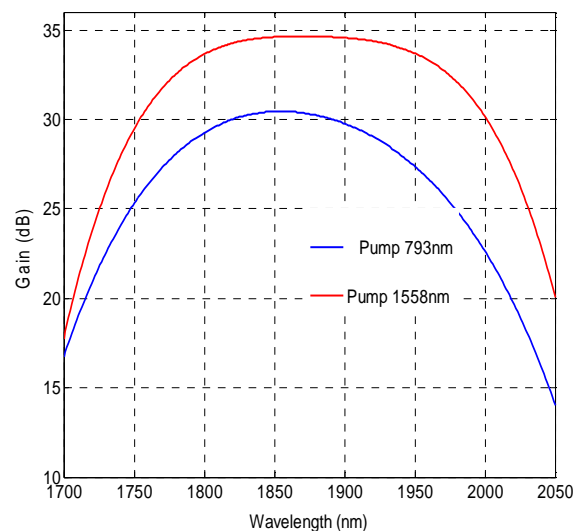


Fig. 7. Signal gain at 1900 nm versus different pump levels for the launched pump wavelengths of 1558 nm and 793 nm.



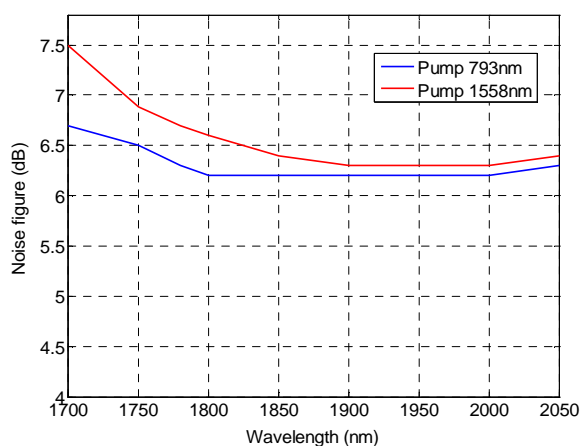


Fig. 8. Noise figure versus seed wavelengths for the launched pump wavelengths of 1558 nm and 793 nm.

#### IV. CONCLUSION

A theoretical model of TDFA operating around 2  $\mu\text{m}$  is built up by solving a set of rate and propagation equations. A MATLAB program is developed with Runge-Kutta method to investigate the static behavior of the TDFA under two pump bands. The proposed model provides the influences of ASE, wavelength and power of the seed, fiber length and pump power in the TDFA performance. This is the first time, to our knowledge, that a theoretical study compares the performance of thulium-doped fiber amplifier around 2  $\mu\text{m}$  for two different pumping schemes.

The simulation results show that the signal gain at the in-band pump is higher than at the indirect pump with the same noise figure around 6 dBm under the same conditions. In case of the in-band pump, the maximum gain reaches to 34.4 dB at 1900 nm seed wavelength with the pump power of 2 W and the signal power of -10 dBm. In contrast to an indirect pump, the maximum gain is only 30 dB under the same conditions. Also it is clearly seen that the TDFA reaches its saturation regime starting from a seed power of -14 dBm at both pump wavelengths. As conclusion TDFA pumped at 1558 nm is more efficient with a core pumped low concentration thulium-doped fiber. Finally, high amplification gain can be achieved when the selected seed wavelengths are near the centre of emission cross-section curve of the thulium doped fiber.

#### REFERENCES

1. K. Thyagarajan and A. Ghatak 'Lasers: Fundamentals and Applications' Springer, USA, 2010.
2. S. W. Henderson, P. J. M. Suni, C. P. Hale, S. M. Hannon, J. R. Magee, D. L. Bruns, and E. H. Yuen, "Coherent laser radar at 2  $\mu\text{m}$  using solid state lasers," IEEE Trans. Geosci. Remote Sens. Vol. 31, no. 1, pp. 4-15, 1993.
3. N. M. Fried, "Thulium fiber laser lithotripsy: An in vitro analysis of stone fragmentation using modulated 110-Watt thulium fiber laser at 1.94  $\mu\text{m}$ ," Lasers Surg. Med. Vol. 37, no. 1, pp. 53-58, 2005.
4. G. J. Koch, J. Y. Beyon, B. W. Barnes, M. Petro, J. Yu, F. Amzajerdian, M. J. Kavaya, and U. N. Singh, "High-energy 2  $\mu\text{m}$  Doppler lidar for wind measurements," Opt. Eng. , vol. 46, no. 11, pp. 116201-116214, 2007.
5. T. Bleuel, M. Brockhaus, J. Koeth, J. Hofmann, R. Werner and A. Forchel, "single-mode DFB lasers for gas sensing in the 2- $\mu\text{m}$  wavelength range," Proc. SPIE 3858, Advanced Materials and Optical Systems for Chemical and Biological Detection, 119 , December 15, 1999.
6. G. Bouwmans, F. Luan, J. C. Knight, P. St. J. Russell, L. Farr, B. J. Mangan, and H. Sabert, "properties of a hollow-core photonic

- band-gap fiber at 850 nm wavelength," Opt. Express, vol. 11, no. 14, pp. 1613-1620, 2003.
7. N. Mac Suibhne, Z. Li, B. Baeuerle and J. Zhao, "WDM Transmission at 2  $\mu\text{m}$  over Low-Loss Hollow Core Photonic Band-gap Fiber," in Optical Fiber Communication Conference/National Fiber Optic Engineers Conference 2013, OSA Technical Digest (online) (OSA, 2013), paper OW11.6.
8. Z. Li, S. U. Alam, J. M. O. Daniel, P. C. Shardlow, D. Jain, N. Simakov, A. M. Heidt, Y. Jung, J. K. Sahu, W. A. Clarkson and D. J. Richardson, "90 nm Gain Extension Towards 1.7  $\mu\text{m}$  for Diode-Pumped Silica-Based Thulium-doped Fiber Amplifiers," in (2014). Paper Tu.3.4.2.
9. Z. Liu, Z. Li and Y. Chen., "52.6Gbit/s Single-Channel Directly-Modulated Optical Transmitter for 2  $\mu\text{m}$  Spectral Region," Optical fiber communication conference, (2015), paper Th1E.6.
10. Y. Wang; H. Po, "Dynamic characteristics of double-clad fiber amplifiers for high-power pulse amplification," J. of Lightwave Technology, vol. 21, no. 10, pp. 2262-2270, 2003.
11. J. E. Crahay, P. Megret, P. Froidure, J. C. Lamquin, and M. Blondel , "Analysis of numerical methods efficiency for EDFA modeling," in Electrotechnical Conference, 1994. Proceedings., 7th Mediterranean I, pp. 12-14, 1994.
12. S. D. Jackson and T. A. King, "Theoretical modeling of Tm-doped silica fiber lasers," J. of Lightwave Technology 17(5), 948-956 (1999).
13. Y. L. Tang and J. Q. Xu, "Effects of excited-state absorption on self pulsing in Tm<sup>3+</sup>-doped fiber lasers," J. Opt. Soc. Am., vol. 27, no.2, pp. 179-186, 2010.
14. F. Wang, D. Shen, H. Chen, D. Fan, and Q. Lu, "Modeling and optimization of stable gain-switched Tm-doped fiber lasers," Optical Review, vol. 18, no. 4, pp. 360-364, 2011.
15. M. Gorjan, T. North, and M. Rochette, "Model of the amplified spontaneous emission generation in thulium-doped silica fibers," J. Opt. Soc. Am. B, vol. 29, no.10, pp. 2886-2890, 2012.
16. Z. Y. Hu, P. Yan, Q. Liu, E. C. Ji, Q. R. Xiao, and M. L. Gong, "High-power single-stage thulium-doped superfluorescent fiber source," Appl. Phys. B, vol. 118, no. 1, pp. 1-7, 2014.
17. G. Yu, J. Chang, Q. Wang, X. Zhang, Z. Liu, and Q. Huang, "A theoretical model of thulium-doped silica fiber's ASE in the 1900 nm waveband," Optoelectron. Lett., vol. 6, no. 1, pp. 45-47, 2010.
18. Z.-Y. Hu, P. Yan, Q.-R. Xiao, Q. Liu, and M.-L. Gong, "227-W output all-fiberized Tm-doped fiber laser at 1908 nm," Chinese Phys. B, vol. 23, no. 10, pp. 104206, 2014.
19. J. Xu, M. Prabhu, J. Lu, K. Ueda, and D. Xing, "Efficient double-clad thulium-doped fiber laser with a ring cavity," Appl. Opt., vol. 40, no. 12, pp. 1983-1988, 2001.
20. S. D. Jackson, "The spectroscopic and energy transfer characteristics of the rare earth ions used for silicate glass fibre lasers operating in the shortwave infrared," Laser Photon. Rev., vol. 3, no. 5, pp. 466-482, 2009.
21. S.D. Emami, S. W. Harun, H.A.A. Rashid and H. Ahmad, "Thulium-Doped Fiber Amplifier, Numerical and Experimental Approach," Nova Science Publishers, Inc., pp. 15-60, 2011.